

Supporting Information

Defined pH-sensitive Nanogels as Gene Delivery Platform for siRNA mediated *in vitro* gene silencing

*Mathias Dimde,^{a[+]} and Falko Neumann,^{a[+]} Felix Reisbeck,^a Svenja Ehrmann,^{a,b} Jose Luis Cuellar-Camacho,^a Dirk Steinhilber,^a Nan Ma,^{*a,c} Rainer Haag^{*a}*

^aInstitute of Chemistry and Biochemistry, Freie Universität Berlin, Takustrasse 3, Berlin 14195, Germany

^bForschungszentrum für Elektronenmikroskopie, Freie Universität Berlin, Fabeckstraße 36A, 14195 Berlin, Germany

^cInstitute of Biomaterial Science and Berlin-Brandenburg Center for Regenerative Therapies Helmholtz-Zentrum Geesthacht, Kantstrasse 55, Teltow 14513, Germany

[+] both authors contributed equally

Table of content

Nanogel size distribution after 2-month storage by DLS

Nanogel height and width calculation by AFM

siRNA loading efficiency

Cell viability measurements in HaCat cells

Cellular uptake in HaCat cells

Flow cytometry results for the GFP-siRNA transfection assay

Red blood cell lysis assay

¹H NMR (pH-sensitive DPG-amine and PEI-acrylamide)

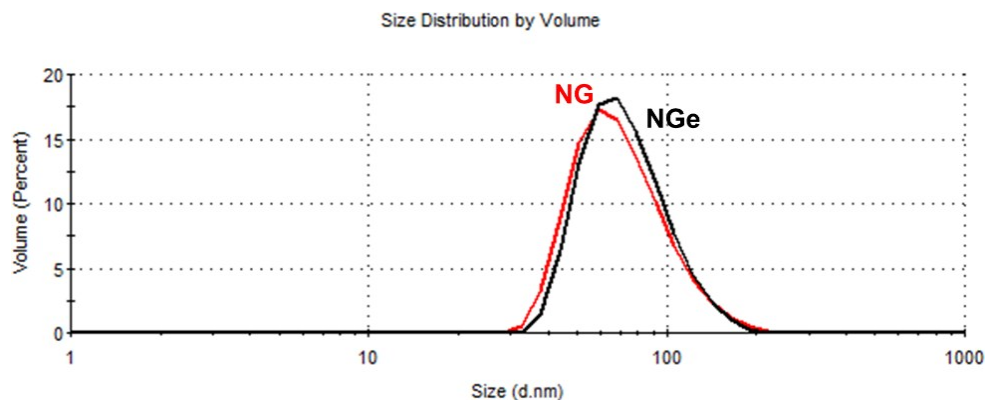


Figure S 1. Size distribution by volume of the pH-sensitive nanogels after two months of storage at 4° C, determined by DLS.

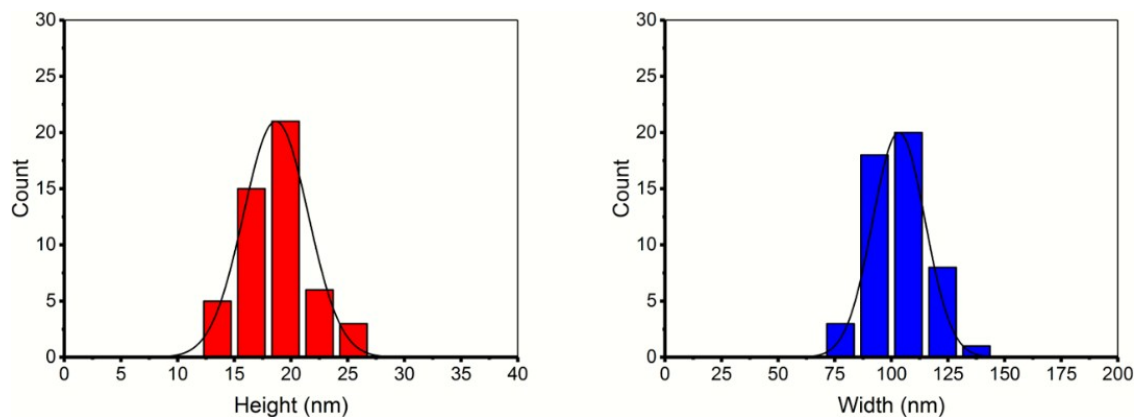


Figure S 2. Nanoparticle height and width measured by AFM.

The nanogel was complexed with various amounts of Alexa Fluor 488 labeled siRNA. The normalized fluorescence intensity of the siRNA complexed with the nanogel was plotted as a function of the siRNA concentration per nanogel (see Figure S3, in blue). In general, 50 pmol siRNA were complexed or encapsulated in 1 mg nanogel (100%). The nanogel with *in situ* encapsulated siRNA (NGe, in orange) complexed 42.61 ± 2.71 pmol siRNA in 1 mg nanogel ($85 \pm 5\%$ encapsulation efficiency).

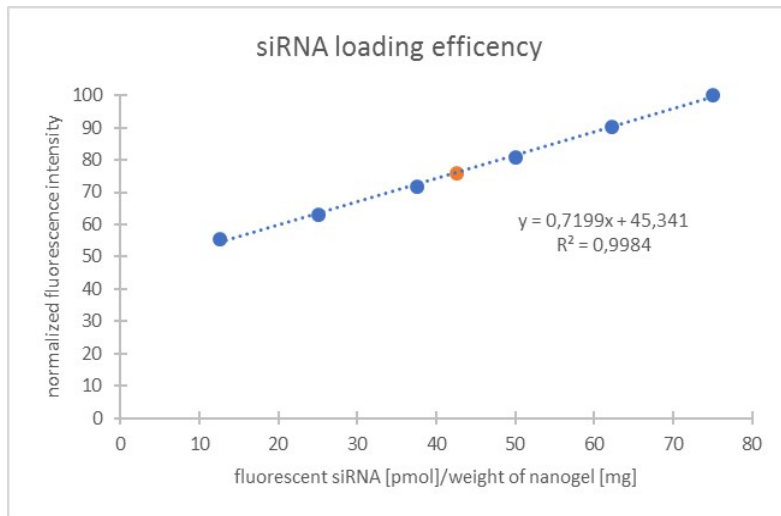


Figure S 3. Calibration curve for the calculation of the siRNA loading efficiency

Cell Viability measurements in HaCat cells yielded similar results compared to the measurements in HeLa cells, solidifying the reduced toxicity of the *low molecular weight* PEI inside the nanogels compared to 25 kDa branched PEI.

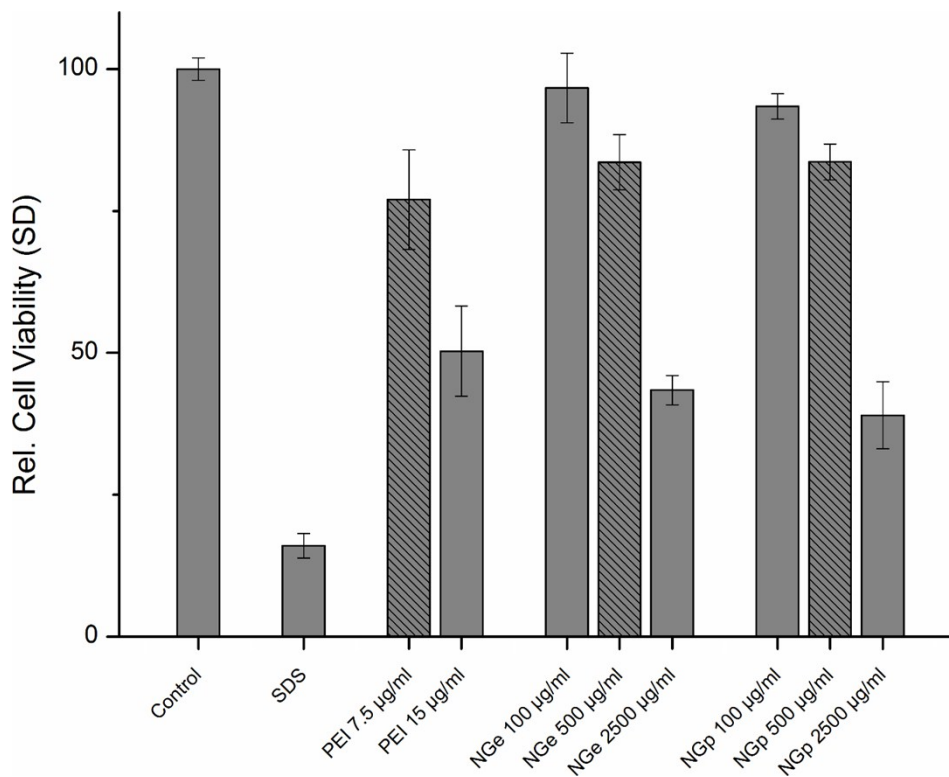


Figure S 4. Cell Viability measurement in HaCat cells after 48 hours. Patterned bars represent concentrations used for transfection studies.

In Figure S5, Alexa Fluor 488 labeled siRNA (green) and rhodamine labeled nanogels (red) were applied on human keratinocytes (nucleus stained in blue). Both components could be found located in the perinuclear region, though a portion of the green siRNA signal can be observed outside of the nanogels. This indicates a slow cargo release as after 24 hours, some of the siRNA is still bound to the nanogels. Free siRNA was not observed to enter the cells.

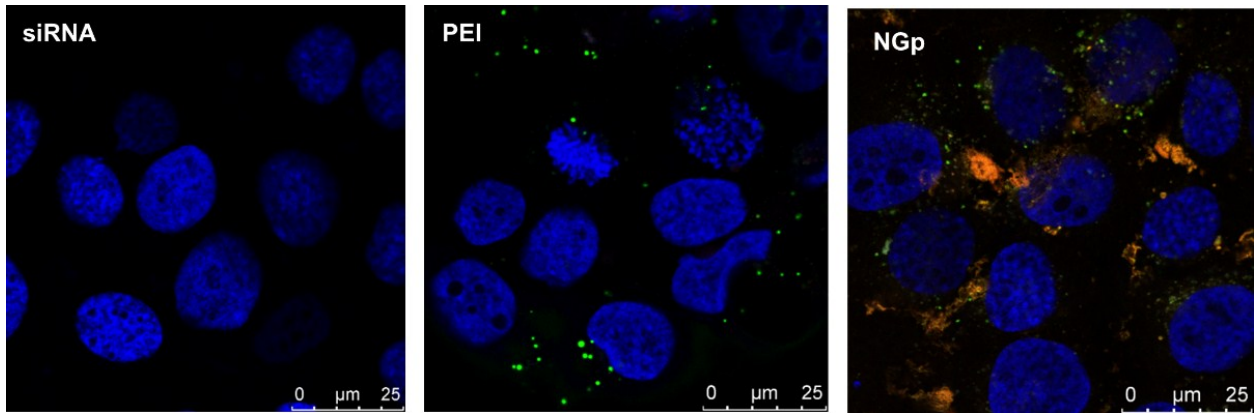


Figure S 5. HaCat cellular uptake observed via confocal microscopy.

In Figure S6, the negative control (NC) shows a narrow peak of uniformly GFP-expressing cells that are negative considered as the baseline. For PEI, a bimodal distribution can be observed as only 13.7% of the cells to continue the same level of GFP expression. For the nanogels (NGp and NGe), more than 70% of cells express a level of GFP smaller than the threshold even though the distribution has only one peak.

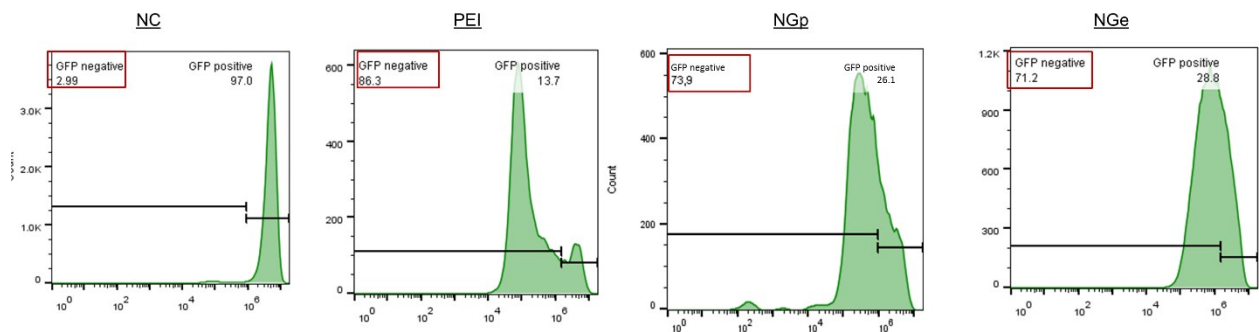


Figure S 6. Flow cytometry results of GFP-siRNA transfection efficiency studies.

Figure S7 shows the results of the red blood cell lysis assay in which cells from a human donor were incubated for one hour with the nanogels (NGe and NGp) and 25 kDa branched PEI. A 20% triton X solution was used as a positive control and showed a very high absorption due to the high hemoglobin content, which was released in the supernatant due to cell lysis. 25 kDa branched PEI at the same concentration as used in the *in vitro* transfection studies showed a minor cell lysis whereas the nanogels did not cause any cell lysis even at five times of the transfection concentrations.

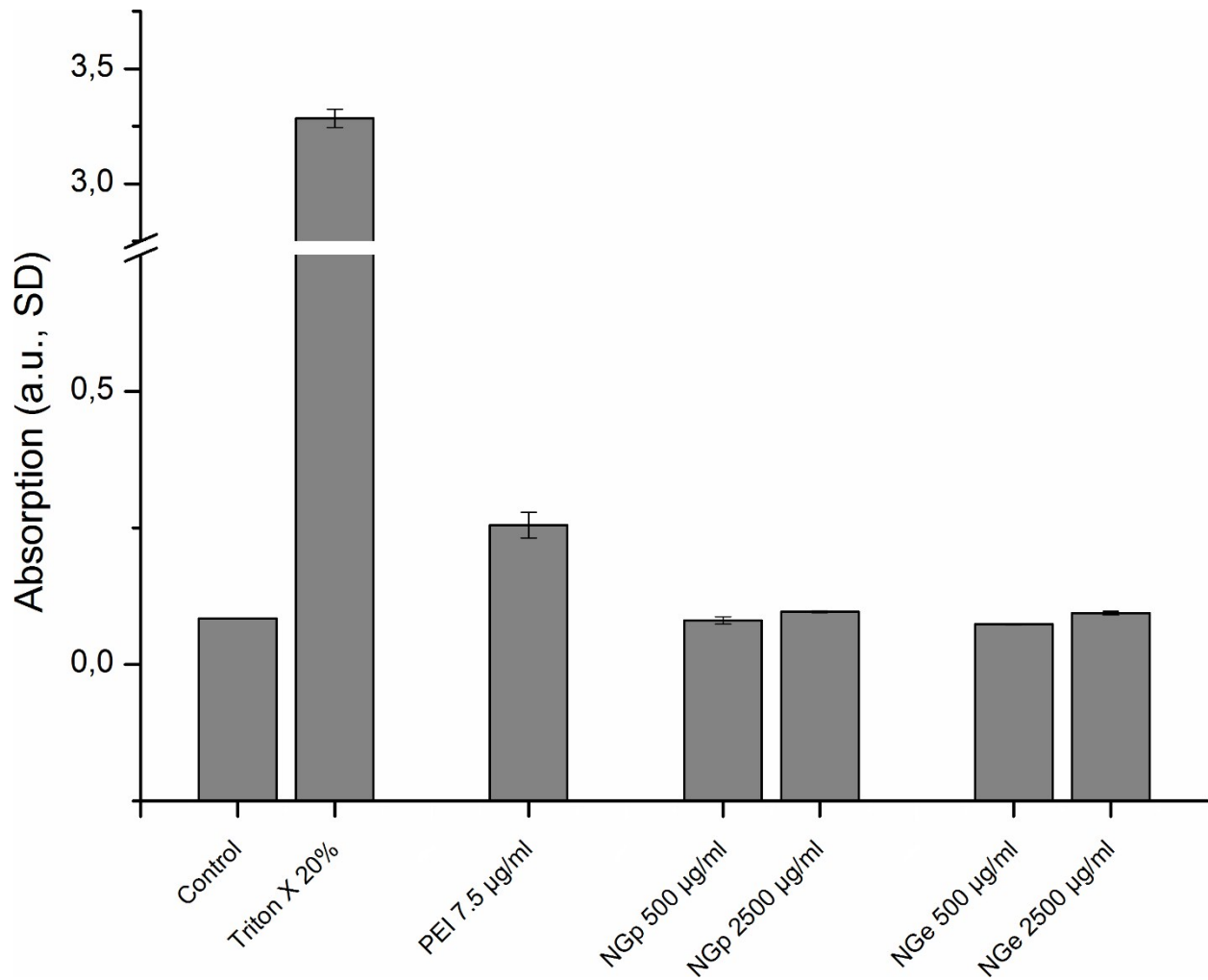


Figure S 7. Red blood cell lysis assay results. Triton X 20% was used as a positive control for 100% of cell lysis.

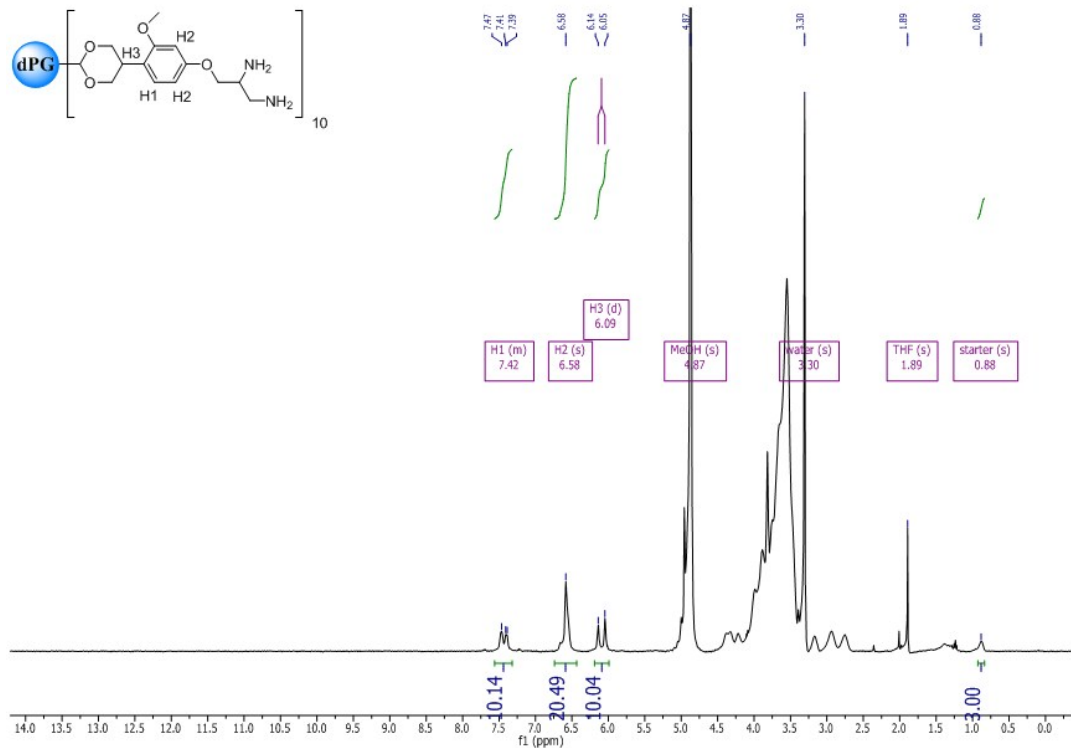


Figure S 8. ^1H NMR of the pH-cleavable dPG-amine

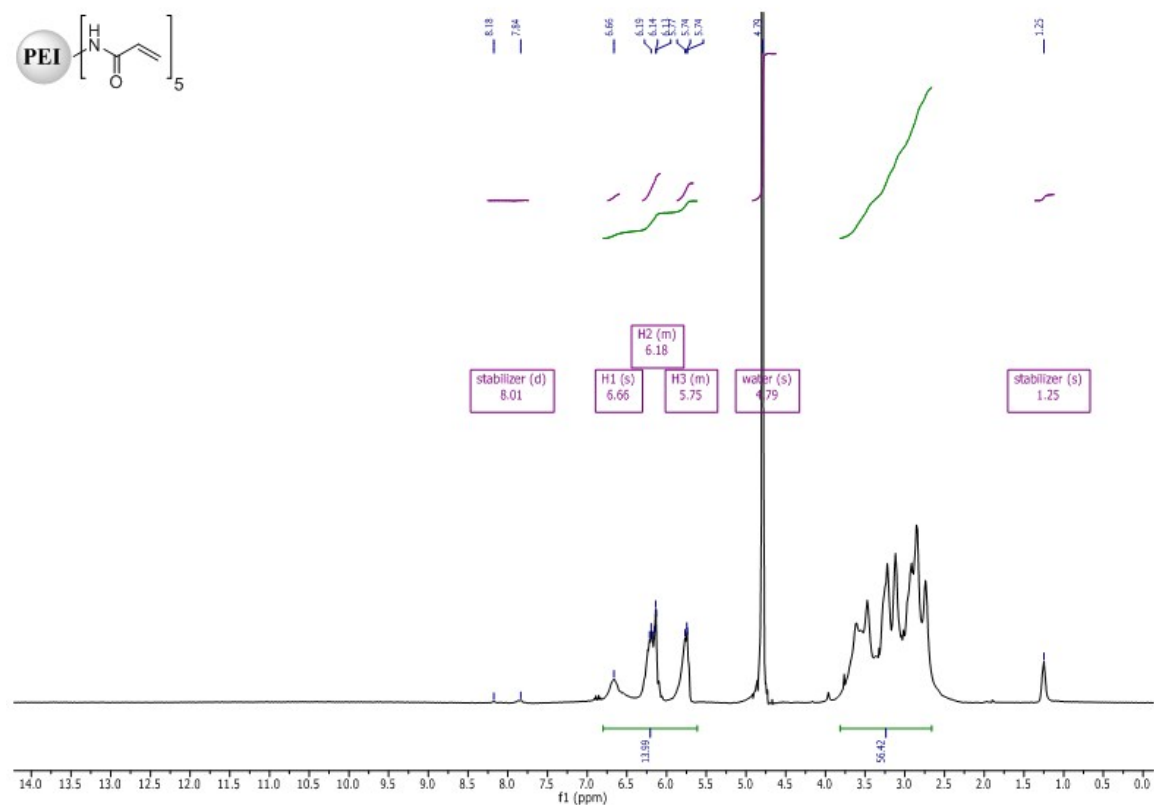


Figure S 9. ^1H NMR of the PEI-acrylamide